Available online at www.sciencedirect.com
SCIENCE DIRECT®
Journal of the European Ceramic Society 25 (2005) 3451–3457
www.elsevier.com/locate/jeurceramsoc

Microwave frequency dielectric properties of hexagonal perovskites in the $Ba_5Ta_4O_{15}$–$BaTiO_3$ system

A.N. Baranov, Young-Jei Oh*

Materials Science and Technology Division, Korea Institute of Science and Technology, Seoul 136-791, South Korea

Received 9 September 2003; received in revised form 16 August 2004; accepted 27 August 2004
Available online 28 October 2004

Abstract

The dielectric properties of the hexagonal perovskites $Ba_8Ta_{4+0.8x}Ti_{3-x}O_{24}$ ($x = 0$, 0.4, and 0.8), $Ba_{10}Ta_{8-0.8x}Ti_xO_{30}$ ($x = 0.6$, 0.9, and 1.2) and $Ba_5Sr_2Ta_4ZrO_{21}$ were studied at microwave frequencies. XRD analysis did not reveal the presence of impurity phases in the obtained samples and the lattice parameters of solid solutions were linearly dependent on composition. These systems show a relatively high permittivity ($27 < \varepsilon < 44$) with a low dielectric loss ($10{,}000 < Q \times f < 31{,}000$ GHz). Solid solutions $Ba_{10}Ta_{8-0.8x}Ti_xO_{30}$ with disordered face-sharing octahedra show higher $Q \times f$ values compared to ordered $Ba_8Ta_{4+0.8x}Ti_{3-x}O_{24}$ compounds. Filling of empty vacancy layers by multicharged cations in the $Ba_5(Ta, Ti)_{4+\delta}O_{15}$ system ($0 < \delta < 1$) along with $Ba_5Sr_2Ta_4ZrO_{21}$ intergrowth leads to decrease a quality factor. The effect of increasing Ti content in the pseudobinary $Ba_5Ta_4O_{15}$–$BaTiO_3$ system on microwave dielectric properties is discussed.

Keywords: Dielectric properties; Perovskites; Tantalates; $Ba_5Ta_4O_{15}$; $BaTiO_3$

1. Introduction

Development of microwave ceramics with a high dielectric constant (ε_r) and good thermal stability together with small dielectric losses in wide temperature and frequency ranges is a key problem in the application of such materials to microwave technology. A combined study of both the crystal structure and the electrophysical properties of new compounds and solid solutions is necessary for the development of new ceramic materials. The dielectric properties of oxides based on the cubic perovskite structure depended on chemical composition, crystal structure and methods of synthesis.[1] The highest Q values have been obtained in ceramics based on ABO_3 perovskite structure where Ta^{5+} cations occupy 2/3 of the B-positions with 1/3 of the positions occupied by Mg^{2+} or Zn^{2+} cation.[1,2] It has been recognized that Q could be enhanced by inducing cation ordering through prolonged sintering at high temperatures.[1,3]

However, there are few reports of the dielectric properties of B-site deficient hexagonal perovskites $AB_{1-x}O_3$ containing mixed cubic/hexagonal stacking sequences. These oxides crystallize as hexagonal perovskites and their crystal structure corresponds to close-packed stacking of AO_3 layers. Stacking sequences can be described using c and h notation where c means cubic stacking with different neighboring layers and h means hexagonal stacking with alike neighboring layers. Accordingly, two types of octahedra are present in these structures—face-sharing octahedra (FSO) and corner-sharing octahedra (CSO). The stability of such cation deficient structures strongly depends on the size and the formal charge of the B-site cations. The need for electroneutrality leads to the appearance of vacancies on the B-sites. For the $A_nB_{n-1}O_{3n}$ homologous series the vacancies are usually ordered between hh layers and structure can be described as alternation of completely filled B-cation layers separated by vacancy layers. This octahedral framework is known for its great ability to accommodate various structural modifications. This possibility is combined with the phenomenal range of catalytic, electronic and magnetic properties.

* Corresponding author. Tel.: +82 2 958 5553; fax: +82 2 958 6720.
E-mail address: youngjei@kist.re.kr (Y.-J. Oh).

0955-2219/$ – see front matter © 2004 Elsevier Ltd. All rights reserved.
doi:10.1016/j.jeurceramsoc.2004.09.010

The microwave dielectric properties of $A_5B_4O_{15}$ ceramics (A = Ba, Sr, Mg, Zn, Ca; B = Nb, Ta) have been determined.[4,5] The best $Q \times f$ values among these hexagonal compounds were obtained for $Ba_5Ta_4O_{15}$ and $Ba_5Nb_4O_{15}$.[6] Increase of $Q \times f$ values at substitution of A-site Ba^{2+} cations with Sr^{2+} in $(Ba_{5-x}Sr_x)Nb_4O_{15}$ has been studied.[7] It has been shown that the Ti-based $La_4Ba_2Ti_5O_{18}$ perovskite with similar hexagonal structure have a low dielectric loss ($Q \times f = 31{,}839$) and high permittivity ($\varepsilon_r = 46$).[8] Recently it was reported about high ($Q \times f = 62{,}000$) value of $Ba_8ZnTa_6O_{24}$ hexagonal perovskite.[9] This compound is isostructural to the $Ba_8ZnTa_6O_{24}$ hexagonal perovskite with eight-layer $(cchc)_2$ close-packed arrangement of BaO_3 layers.[10]

In the $Ba_5Ta_4O_{15}$–$BaTiO_3$ system two types of solid solution—$Ba_8Ta_{4+0.8x}Ti_{3-x}O_{24}$ and $Ba_{10}Ta_{8-0.8x}Ti_xO_{30}$ have been detected. These solid solutions have two types of FSO with different occupancies of the vacancy layer by Ta atoms, Ti atoms and vacancies, which result in formation of a superstructure. In the $Ba_{10}Ta_{8-0.8x}Ti_xO_{30}$ structures FSO also occur in a disordered fashion and in the $Ba_8Ta_{4+0.8x}Ti_{3-x}O_{24}$ structure in an ordered fashion.[11] Compounds in the $Ba_5Ta_4O_{15}$–$BaZrO_3$ system also form intergrowth structures with alternating $Ba_5Ta_4O_{15}$-type and $BaZrO_3$-type structural blocks.[12] These $Ba_5Ta_4O_{15}$–$BaTiO_3$ (BTT) systems are of interest as model systems for the study of microwave dielectric properties of B-site substituted hexagonal perovskites with varying types of order.

In this paper microwave dielectric properties of $Ba_8Ta_{4+0.8x}Ti_{3-x}O_{24}$ ($x = 0$, 0.4, and 0.8) and $Ba_{10}Ta_{8-0.8x}Ti_xO_{30}$ ($x = 0.6$, 0.9, and 1.2) solid solutions of hexagonal perovskites and $Ba_5Sr_2Ta_4ZrO_{21}$ composition, were investigated. The influence of substitution of Ta^{5+} by Ti^{4+} in the $Ba_5Ta_4O_{15}$ "parent" compound in the pseudobinary $Ba_5Ta_4O_{15}$–$BaTiO_3$ system on microwave dielectric properties is discussed.

2. Experimental procedures

All studied samples were prepared by a solid-state synthesis technique using $BaCO_3$, Ta_2O_5 and TiO_2 as initial reagents. Stoichiometric amounts of the powders were ball milled using zirconia balls in plastic containers for 24 h in deionized water. The pelletized samples were preheated to 1000 °C for 40 h. The calcined tablets were crushed, ball milled again, mixed with 2 drops of 5 wt.% solution of polyvinylalcohol (PVA) as binder, and uniaxially pressed in cylindrical disks with 10 mm diameter and 7 mm height under pressure of 200 MPa. The samples were fired 40 h at 1400 °C on air with two intermediate exposures during heating for 1 and 2 h at 350 and 1000 °C, respectively, for removing the binder and traces of barium carbonates. The sintered samples were well polished and their bulk density was measured using Archimedes method. The morphology of the samples was examined by scanning electron microscopy (FE-SEM; Hitachi S-4200 SEM). The decomposition of the precursor powders was studied by thermal gravimetric analysis (TGA) on air in platinum crucible using thermogravimetric analyzer (Universal V1.8M TA Instruments). The crystal structure and phase purity of the samples were studied by X-ray diffraction techniques. X-ray powder diffraction (XRD) data of the synthesized samples were collected by a Rigaku RINT DMAX 2500 diffractometer (Cu Kα radiation). All peaks for the composition #1–3 match with $Ba_8Ta_4Ti_3O_{24}$ compound (S.G. $P6_3/mmc$ (194); JCPDS card 44-0264) and for composition #4–6 with $Ba_{10}Ta_{7.04}Ti_{1.2}O_{30}$ compound (S.G. $P6_3/mmc$ (194); JCPDS card 44-0561). The lattice parameters of the samples were calculated by the least-square fitting method (Table 1). Specimens were examined using a PHILLIPS CM30 TEM operated at 200 kV. Thin foils for TEM were prepared by the conventional technique of slicing the annealed samples using a diamond saw, ultrasonic cutting to discs of 3 mm in diameter, mechanical polishing using SiC grits, dimple grinding (Gatan Dimple grinder) and

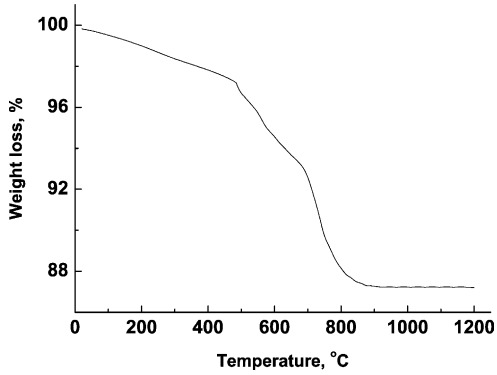

Fig. 1. TGA curve of the ball-milled precursor—mixture of $BaCO_3$, Ta_2O_5 and TiO_2 with 5% PVA binder (composition #1).

Table 1
Lattice parameters of BTT samples calculated from XRD diffractograms

Sample no.	Composition	x	a (Å)	c (Å)	a (Å) (Ref. 11)	c (Å) (Ref. 11)
1	$Ba_8Ta_{4+0.8x}Ti_{3-x}O_{24}$	0	5.7882	18.833	5.7913(1)	18.8710(7)
2		0.4	5.7942	18.879		
3		0.8	5.8033	18.898	5.8038(9)	18.912(5)
4	$Ba_{10}Ta_{8-0.8x}Ti_xO_{30}$	1.2	5.7965	23.767	5.7966(1)	23.7482(7)
5		0.9	5.8008	23.802		
6		0.6	5.8027	23.817	5.8056(5)	23.860(3)

Table 2
Microwave dielectric properties of synthesized samples

Sample no.	Compound	x	δ	ε_r	Q	$Q \times f_0$ (GHz)	$\tau_f \times 10^6$ (ppm/°C)	d (%TD)
1	$Ba_8Ta_{4+0.8x}Ti_{3-x}O_{24}$	0	0.5	40	1735	12960	–	96
2		0.4	0.46	36	1585	12050	–	92
3		0.8	0.42	44	1187	9720	–	97
4	$Ba_{10}Ta_{8-0.8x}Ti_xO_{30}$	1.2	0.12	35	3411	25760	64	92
5		0.9	0.09	35	3105	23640	69	93
6		0.6	0.06	34	4019	30820	57	94
7	$Ba_5Ta_4O_{15}$ [4]		0	28	5700	31640	12	95
8	$Ba_5Sr_2Ta_4ZrO_{21}$			27	1282	9810		92

ion-beam thinning (Duomill™ 600, Gatan, Pleasanton, CA, USA) to electron transparency. Composition microanalysis for the BTT grains was performed via energy dispersive X-ray spectroscopy (EDS) using (EDAX, DX-4, Mahwah, NJ, USA) equipped with TEM and the crystals were found to have a composition close to the nominal one.

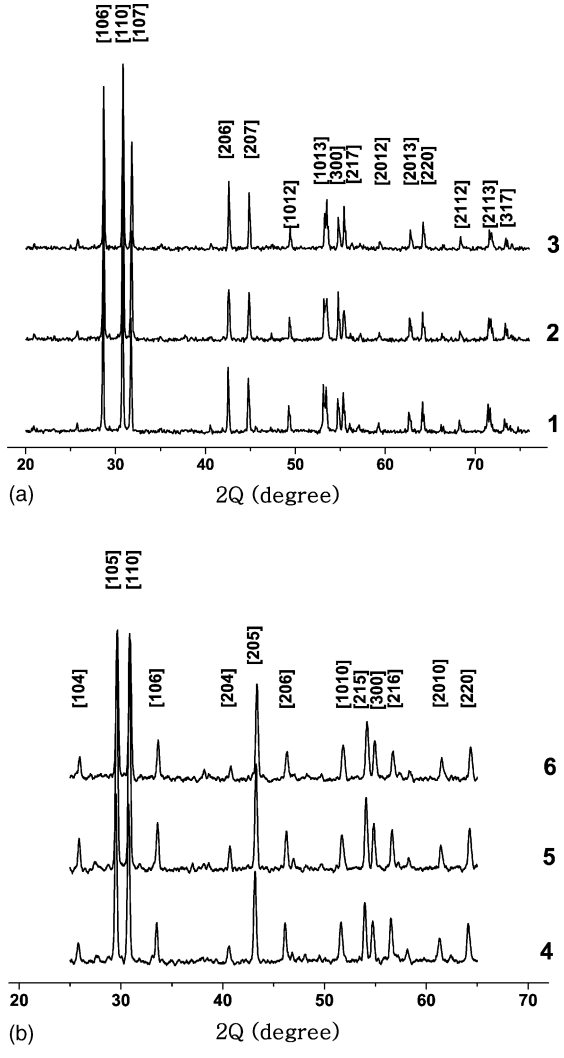

Fig. 2. (a) XRD spectra for the samples #1–3 with $Ba_8Ta_{4+0.8x}Ti_{3-x}O_{24}$ ($x = 0$, 0.4, and 0.8) composition. (b) XRD spectra for the samples #4–6 $Ba_{10}Ta_{8-0.8x}Ti_xO_{30}$ ($x = 1.2$, 0.9, and 0.6) composition.

The dielectric constant was measured by Hakki and Coleman's dielectric-resonator method at microwave frequency. The quality factor was measured by a reflection system at resonant frequency using a network analyzer (Hewlett Packard, Model HP 8720C). For the present samples resonance occurred between 5.5 and 8.5 GHz. The temperature coefficient of resonant frequency was measured by noting the variation of TE_{011} resonance mode in the temperature range 25–80 °C.

3. Results and discussion

For accurate evaluation of microwave dielectric properties in a series of solid solutions, high dense (>95%) and single-phase ceramics with similar microstrucure should be prepared. The sintering technique that was used for preparing single-phase samples in refs. 11 and 12 produced porous ceramics not suitable for dielectric measurements. To avoid melting and formation of secondary phases sintering temperature was kept below 1400 °C. Generally, densification is being promoted by intermediate milling of the calcined powders. Instead, consequent regrinding and sintering of the samples at 1400 °C have led to the saturation of relative density at less than 90% value.

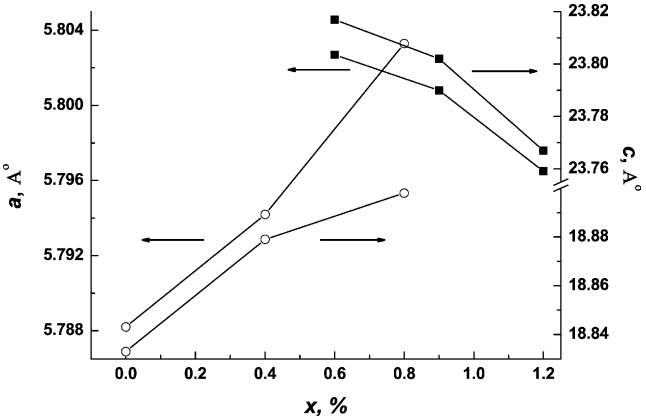

Fig. 3. Lattice parameters of the samples #1–6 vs. x. Open circles: samples #1–3; dark squares: samples #4–6.

TGA curve for Ba–Ta–Ti–O (BTT) precursor, given in Fig. 1, is typical for all Ba–Ta–Ti–O samples. The weight loss at $T < 500\,^{\circ}C$ can be attributed to the removal of absorbed water and decomposition of PVA binder.[13] Two-stage process at 500–900 °C deals with decomposition of barium carbonate and formation of complex oxide. XRD analysis of samples calcined at 1000 °C proved that formation of the $Ba_{10}Ta_{8-0.8x}Ti_xO_{30}$ and $Ba_8Ta_{4+0.8x}Ti_{3-x}O_{24}$ main phases is completed at this temperature, as no impurity phases are present in the X-ray patterns. The temperature treatment of the ball-milled precursors was optimized based on TGA results to get the highest density values. First heating up to 350 °C with 10 °C/min rate and soaking for 1 h leads to the binder eliminating, then heating up to 1000 °C with 5 °C/min rate and 2 h soaking results in residual barium carbonate decomposition and phase formation. Cooling was carried out

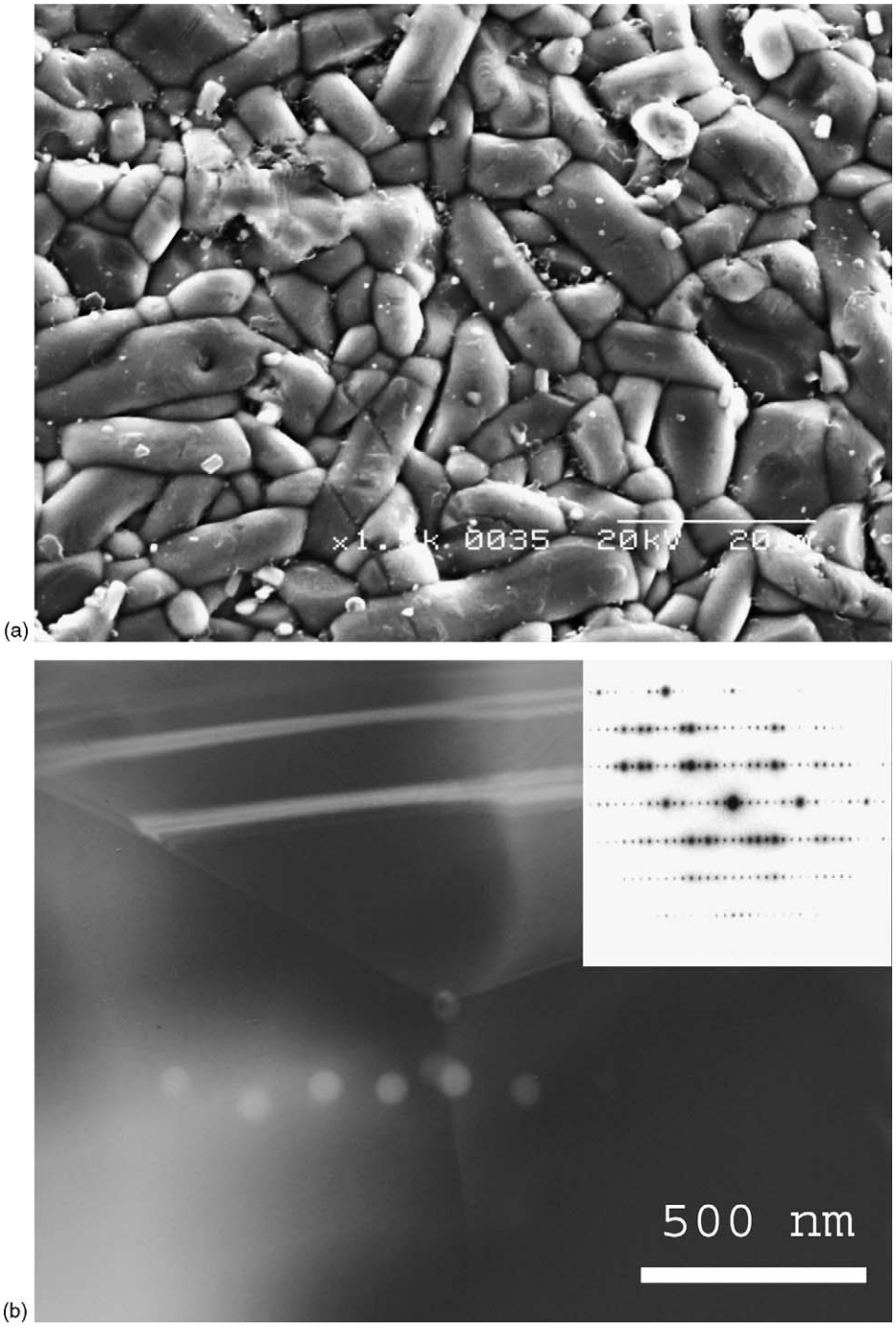

Fig. 4. (a) Typical SEM images of synthesized BTT sample #4, $Ba_{10}Ta_{7.04}Ti_{1.2}O_{30}$ composition. (b) TEM micrograph of sample #1. White spots indicate points of EDS analysis. Inset: Electron diffraction pattern taken from sample #1 along [1 0 0].

with the furnace. Densities of the as-prepared samples (see Table 2) were high enough for microwave dielectric measurements.

Fig. 2a and b show the X-ray diffraction patterns of BTT as-synthesized samples. The calculated by the least-square fitting method lattice parameters are plotted versus x in Fig. 3. The lattice parameters of solid solutions are linearly dependent on the x. For comparison literature values[11] for some compositions are also listed in Table 1, revealing good agreement. The typical SEM micrograph of as-prepared BTT ceramics is shown in Fig. 4a. Dense and non-porous microstructure with rather large grain size of 10–20 μm makes obvious good quality of samples for the microwave dielectric measurements.

The general microstructure of the BTT ceramics was confirmed by TEM analysis (Fig. 4b). The TEM micrograph of the sample #1 shows absence of pores or precipitates either in the matrix or grain boundaries. In some cases twins are observed in large grains (upper part of Fig. 4b). These defects are typical for this structure and their origin was discussed earlier.[11] Quantitative X-ray analysis of BTT grains was performed by EDS analysis, located inside the matrix BTT grains, grain boundaries or in the triple junction. Points of analysis are shown on Fig. 4b as a white spots. Since the $K\alpha$ peaks of titanium strongly overlap the $L\alpha$ peaks of barium, tantalum concentration and sum of titanium and barium concentration were compared. Maximum deviation from the nominal composition does not exceed 1 at.%. Electron diffraction analysis confirms that the $Ba_8Ta_4Ti_3O_{24}$ has the ordered hexagonal structure (inset Fig. 4b) in accordance with the previous research[11] and no crystalline secondary phases were identified.

As it can be seen from Table 2 and Fig. 5; the microwave dielectric properties in each series of Ba–Ta–Ti–O solid solutions vary through a small range, but the difference between series is obvious. The maximum $Q \times f$ value achieved in this study was 30,820 GHz for the $Ba_{10}Ta_{7.52}Ti_{0.6}O_{30}$ composition. As for dielectric constant the highest value 44 was for the $Ba_8Ta_{4.64}Ti_{2.2}O_{24}$ composition.

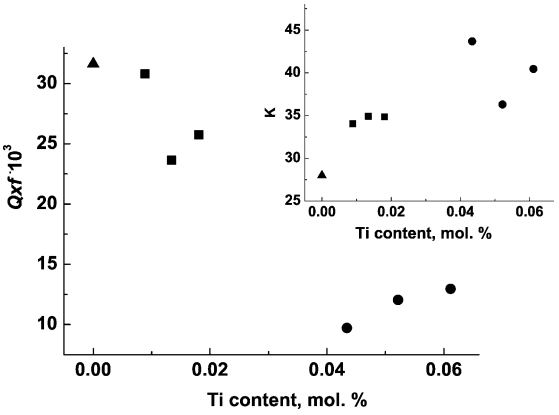

Fig. 5. Microwave dielectric properties ($Q \times f$) of synthesized samples vs. titanium content. Triangles: $Ba_5Ta_4O_{15}$; squares: samples #4–6 ($Ba_{10}Ta_{8-0.8x}Ti_xO_{30}$); and circles: samples #1–3 ($Ba_8Ta_{4+0.8x}Ti_{3-x}O_{24}$) Inset: Dielectric constant (ε_r) of synthesized samples vs. Ti content.

In the $Ba_5Ta_4O_{15}$–$BaTiO_3$ solid solutions substitution Ta^{5+} by Ti^{4+} can be represented as $Ba_5(Ta, Ti)_{4+\delta}O_{15}$ or $A_nB_{n-1+\delta}O_{3n}$. In the series $Ba_5Ta_4O_{15} \rightarrow Ba_{10}Ta_{8-0.8x}Ti_xO_{30} \rightarrow Ba_8Ta_{4+0.8x}Ti_{3-x}O_{24} \rightarrow BaTiO_3$ the value δ (Table 2) reflects increasing of the titanium content and quality factor decreases in these series. As for dielectric constant the dependence on Ti-content has inverse type (see inset in Fig. 5) and increase in Ti-content leads to the increase of dielectric constant. This fact is in agreement with well-known correlation of intrinsic loss with the permittivity by a power law.[1]

All the samples have the same chemical and thermal prehistory. As is suggested by SEM, TEM, and density measurement they have similar dense microstructure. XRD and electron diffraction patterns of the samples do not show presence of any crystalline impurities. Hence the main sources of extrinsic losses in the ceramic samples wholly or in part were minimized. It is reasonable to look at structural changes in the "parent" $Ba_5Ta_4O_{15}$ compound on doping by $BaTiO_3$ and $SrZrO_3$ considering intrinsic losses in series of solid solutions.

$Ba_5Ta_4O_{15}$ crystallizes in the $P3\bar{m}1$ space group and has trigonal structure with a five-layer closest packing with (hccch) stacking sequence (Fig. 6a). The tantalum ions, located in the octahedral holes between layers and cation vacancies, form central layer thus providing charge neutrality and the maximum partition of Ta^{5+} ions. Substitution of $4Ta^{5+}$ by $5Ti^{4+}$ cations requires accomodation of additional multicharged cations on doping. It results in filling of empty vacancy layer and changes in the crystal structure. The crystal structure of $Ba_{10}Ta_{7.04}Ti_{1.2}O_{30}$ is based on the 10H $(hcccc)_2$ close packing of BaO_3 layers (Fig. 6b) and two types of corner-sharing octahedra are present. All of them are jointly occupied by Ta and Ti atoms. The B-site cations occupy 1/4 of the octahedral cavities existing between AO_3 layers in such a way that the BO_6 octahedra form a 3D network of corner-sharing octahedra (CSO). Replacement of Ta by Ti cations leads not only to the occupancy of vacancy layer empty in $Ba_5Ta_4O_{15}$. Distance between the nearest Ta–Ta atoms becomes 2.34 Å that corresponds to a metal-metal bond. Strong anisotropy of the thermal parameters indicates a cationic displacement of some Ta cations from ideal position allowing to extension of the Ta–Ta distance. These deviations from the perfect lattice periodicity lead to scattering of the phonons and thus to dielectric losses.[1] Close occupancy of two types of FSO ((0.5Ta + 0.5) and 0.56(Ta, Ti) + 0.44) suggests disordered arrangement of different pairs of FSO.[11]

The crystal structure of $Ba_8Ta_{4+0.8x}Ti_{3-x}O_{24}$ is based on the 8H $(cchc)_2$ close-packed stacking (Fig. 6c). Increasing of Ti content results in the rise of the average occupancy in the second type of FSO (0.875(Ta, Ti) + 0.125). For this reason ordering of FSO has been made possible. Both structures of studied solid solutions contain two types of

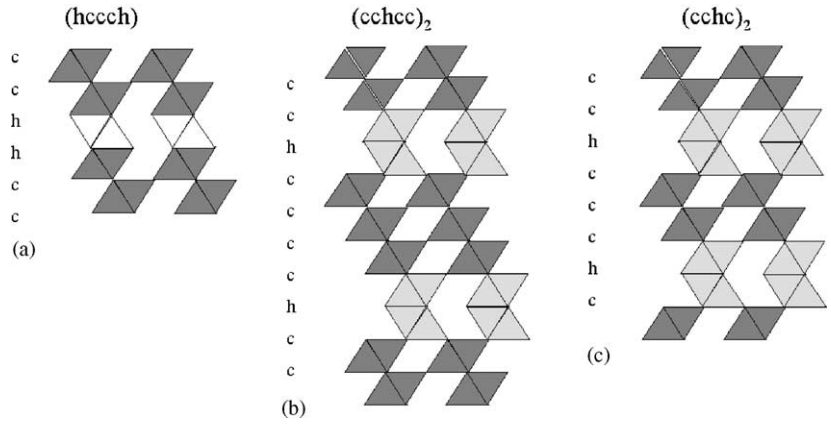

Fig. 6. The stacking sequences (c: cubic and h: hexagonal) for (a) $Ba_5Ta_4O_{15}$, (b) $Ba_{10}Ta_{8-0.8x}Ti_xO_{30}$, and (c) $Ba_8Ta_{4+0.8x}Ti_{3-x}O_{24}$ compounds. Dark triangles: B-site fully occupied; light dark triangles: B-site partially occupied; and light triangles: B-site empty.

face sharing octahedras (FSO) with different occupancies by Ta atoms, Ti atoms and vacancies. Structures of $Ba_8Ta_{4+0.8x}Ti_{3-x}O_{24}$ and $Ba_{10}Ta_{8-0.8x}Ti_xO_{30}$ compositions are close to each other but the latter is characterized as more disordered. As for dielectric microwave properties the strengthening of interaction between multicharged Ta^{5+} or Ti^{4+} cations is more significant than ordering and finally resulting in decrease of quality factor in the $Ba_5Ta_4O_{15}$–$Ba_{10}Ta_{8-0.8x}Ti_xO_{30}$–$Ba_8Ta_{4+0.8x}Ti_{3-x}O_{24}$ series. Rather poor microwave dielectric properties of the last studied $Ba_5Sr_2Ta_4ZrO_{21}$ composition indirectly prove this idea.

The crystal structure of $Ba_5Sr_2Ta_4ZrO_{21}$ that can be written as $Ba_5Ta_4O_{21}$–$2SrZrO_3$ consists of chhc lamellae separated by three close-packed layers.[12] In this case insertion of $SrZrO_3$ (ccc) structural blocks leads to intergrowth structure keeping vacancy layer unoccupied. At the same time two FSO should be completely filled by B cations. The placement of highly charged cations with such a short separation (2.36 Å) should destabilize this structure due to a strong electrostatic repulsion. Indeed as it can be seen from Table 2, such consequent filling of FSO leads to the deterioration of quality factor from $Ba_5Ta_4O_{21}$ to $Ba_5Sr_2Ta_4ZrO_{21}$.

4. Conclusions

The microwave dielectric properties of the hexagonal perovskite oxides $Ba_8Ta_{4+0.8x}Ti_{3-x}O_{24}$ ($x = 0$, 0.4, 0.8) and $Ba_{10}Ta_{8-0.8x}Ti_xO_{30}$ ($x = 0.6$, 0.9, 1.2) have been investigated. The maximum $Q \times f$ value achieved in this study was 30,820 GHz for the composition $Ba_{10}Ta_{7.52}Ti_{0.6}O_{30}$. A single-phase ceramic samples having hexagonal perovskite structure has been obtained with high relative density. Solid solutions of $Ba_{10}Ta_{8-0.8x}Ti_xO_{30}$ composition with disordered face-sharing octahedras show better microwave dielectric properties in comparison with ordered $Ba_8Ta_{4+0.8x}Ti_{3-x}O_{24}$ compounds. In the series of $Ba_5Ta_4O_{15}$–$Ba_{10}Ta_{8-0.8x}Ti_xO_{30}$–$Ba_8Ta_{4+0.8x}Ti_{3-x}O_{24}$ compounds dielectric constant is increased in parallel with decreasing of quality factor.

References

1. Wersing, W., Microwave ceramics for resonators and filters. *Curr. Opin. Solid State Mater. Sci.*, 1996, **1**, 715–731.
2. Fang, Y., Hua, A., Ouyang, S. and Oh, Y. J., The effect of calcination on the microwave dielectric properties of $Ba(Mg_{1/3}Ta_{2/3})O_3$. *J. Eur. Ceram. Soc.*, 2001, **21**, 2745–2750.
3. Qazi, I., Reaney, I. M. and Lee, W. E., Order–disorder phase transition in $Ba(Zn_{1/3}Ta_{2/3})O_3$. *J. Eur. Ceram. Soc.*, 2001, **21**, 2613–2616.
4. Kamba, S., Petzelt, J., Buixaderas, E., Haubrich, D., Vanek, P., Kuzˇel, P. *et al.*, High frequency dielectric properties of $A_5B_4O_{15}$ microwave ceramics. *J. Appl. Phys.*, 2001, **89**, 3900–3906.
5. Jawahar, I. N., Mohanan, P. and Sebastian, M. T., $A_5B_4O_{15}$ (A = Ba, Sr, Mg, Ca, Zn; B = Nb, Ta) microwave dielectric ceramics. *Mater. Lett.*, 2003, **57**, 4472–4477.
6. Kim, D. W., Kim, J. R., Yoon, S. H., Hong, K. S. and Kim, C. K., Microwave dielectric properties of low-fired $Ba_5Nb_4O_{15}$. *J. Am. Ceram. Soc.*, 2002, **85**, 2759–2762.
7. Sreemoolanadhan, H., Sebastian, M. T. and Mohanan, P., High permittivity and low loss ceramics in the BaO–SrO–Nb_2O_5 system. *Mater. Res. Bull.*, 1996, **31**, 431–437.
8. Vineis, C., Davies, P. K., Negas, T. and Bell, S., Microwave dielectric properties of hexagonal perovskites. *Mater. Res. Bull.*, 1996, **31**, 431–437.
9. Davies, P. K., Borisevich, A. and Thirumal, M., Communicating with wireless perovskites: cation order and zinc volatilization. *J. Eur. Ceram. Soc.*, 2003, **23**, 2461–2466.
10. Abakumov, A. M., Van Tendeloo, G., Scheglov, A. A., Shpanchenko, R. V. and Antipov, E. V., The crystal structure of $Ba_8Ta_6NiO_{24}$: cation ordering in hexagonal perovskites. *J. Solid State Chem.*, 1996, **125**, 102–107.
11. Shpanchenko, R. V., Nistor, L., Van Tendeloo, G., Van Landuyt, J., Amelinckx, S., Abakumov, A. M. *et al.*, Structural studies on new ternary oxides $Ba_8Ta_4Ti_3O_{24}$ and $Ba_{10}Ta_{7.04}Ti_{1.2}O_{30}$. *J. Solid State Chem.*, 1995, **114**, 560–574.

12. Abakumov, A. M., Shpanchenko, R. V., Antipov, E. V., Lebedev, O. I., Van Tendeloo, G. and Amelinckx, S., Synthesis and structural study of hexagonal perovskites in the $Ba_5Ta_4O_{15}$–$MZrO_3$ (M = Ba, Sr) system. *J. Solid State Chem.*, 1998, **141**, 492–499.

13. Baklouti, S., Bouaziz, J., Chartier, T. and Baumard, J.-F., Binder burnout and evolution of the mechanical strength of dry-pressed ceramics containing poly(vinyl alcohol). *J. Eur. Ceram. Soc.*, 2001, **21**, 1087–1092.